Ultra-high speed OCT allows measurement of intraocular pressure, corneal geometry, and corneal stiffness using a single instrument

Manmohan Singh[a], Zhaolong Han[b], Achuth Nair[a], Alexander Schill[a], Michael D. Twa[c,d], and Kirill V. Larin[a,e,f,*]

[a]Department of Biomedical Engineering, University of Houston, Houston, TX, USA; [b]School of Naval Architecture, Ocean and Civil Engineering, Shanghai Jiao Tong University, Shanghai, China; [c]School of Optometry, University of Alabama at Birmingham, Birmingham, AL, USA; [d]Department of Biomedical Engineering, University of Alabama at Birmingham, Birmingham, AL, USA; [e]Interdisciplinary Laboratory of Biophotonics, Tomsk State University, Tomsk, Russia; [f]Molecular Physiology and Biophysics, Baylor College of Medicine, Houston, TX, USA

*klarin@uh.edu

ABSTRACT

Screening for ocular diseases, such as glaucoma and keratoconus, includes measuring the eye-globe intraocular pressure (IOP) and corneal biomechanical properties. However, currently available clinical tools cannot quantify corneal tissue material parameters, which can provide critical information for detecting diseases and evaluating therapeutic outcomes. Here, we demonstrate measurement of eye-globe IOP, corneal elasticity, and corneal geometry of *in situ* porcine corneas with a technique termed applanation optical coherence elastography (Appl-OCE) with single instrument. We utilize an ultrafast phase-sensitive optical coherence tomography system comprised of a 4X buffered Fourier domain mode-locked swept source laser with an A-scan rate of ~1.5 MHz and a 7.3 kHz resonant scanner. The IOP was measured by imaging the response of *in situ* porcine corneas to a large force air-puff. As with other noncontact tonometers, the time when the cornea was applanated during the inwards and outwards motion was correlated to a measure air-pressure temporal profile. The IOP was also measured with a commercially available rebound tonometer for comparison. The stiffness of the corneas was assessed by directly imaging and analyzing the propagation of a focused micro air-pulse induced elastic wave, and the corneal geometry was obtained from the OCT structural image. Our results show that corneal thickness decreased as IOP increased, and that corneal stiffness increased with IOP. Moreover, the IOP measurements made by Appl-OCE were more closely correlated with the artificially set IOP than the rebound tonometer, demonstrating the capabilities of Appl-OCE to measure corneal stiffness, eye-globe IOP, and corneal geometry with a single instrument.

Keywords: Ocular diseases, keratoconus, glaucoma, optical coherence tomography, optical coherence elastography

1. INTRODUCTION

Screening for ocular diseases, such as keratoconus [1] and glaucoma [2], typically entails measuring corneal geometry, eye-globe intraocular pressure (IOP), and corneal biomechanical properties. For example, a hallmark of pathological keratoconus is a weak and thin cornea [3], and glaucoma is well correlated with an elevated IOP [2]. However, currently available clinical tools lack the ability to truly quantify corneal tissue material parameters, which can provide critical information for detecting diseases and evaluating the outcome of therapeutic procedures. Moreover, corneal biomechanical properties, eye-globe IOP, and corneal geometry are inter-related [4-7], so decoupling these parameters may not be entirely possible. Therefore, there is a need for a technique that can provide quantitative measurements of these critical parameters. Traditional elastographic techniques, such as ultrasound elastography [8] and magnetic resonance elastography [9] are proven powerful clinical tools. However, they require contact for excitation and have poor spatial resolution, which limits their applications for thin samples such as the cornea. Similarly, the "gold standard" of mechanical testing is contact-based and destructive, limiting its usefulness for corneal applications. Brillouin microscopy shows promise for microscale mapping of corneal biomechanical properties [10, 11], but the link between the Brillouin shift and quantitative material parameters is still unknown. Optical coherence

Optical Coherence Tomography and Coherence Domain Optical Methods in Biomedicine XXII, edited by Joseph A. Izatt, James G. Fujimoto, Valery V. Tuchin, Proc. of SPIE Vol. 10483, 1048319 · © 2018 SPIE · CCC code: 1605-7422/18/$18 · doi: 10.1117/12.2288450

tomography [12] based elastography, which is termed optical coherence elastography (OCE) [13, 14], is a powerful elastographic technique that overcomes the limitations of the aforementioned techniques. When combined with noncontact excitation and phase-sensitive detection, OCE can provide noncontact elastographic evaluation of the biomechanical properties of tissues.

In this work, we demonstrate measurement of the eye-globe IOP, corneal elasticity, and corneal geometry with a technique termed applanation optical coherence elastography (Appl-OCE) that only needs a single instrument. Our results on *in situ* porcine corneas show that corneal thickness decreased as IOP increased, and that corneal stiffness increased with IOP. Moreover, the IOP as measured by Appl-OCE was better correlated with the artificially set IOP as compared to a commercially available rebound tonometer.

2. METHODS

Fresh whole porcine eye-globes (n = 3) were obtained fresh (Sioux-Preme Packing Co., IA, USA) and placed in a custom holder to prevent movement and for artificial IOP control. The eye-globes were cannulated with two needles. One needle was connected via tubing to a pressure transducer and the other needle was connected via tubing to a micro infusion pump. The system was controlled by Matlab (MathWorks, MA, USA) to form a close-loop feedback system [15].

A schematic of the experimental setup is shown in Fig. 1. The ultrafast phase-sensitive optical coherence tomography (PhS-OCT) system was comprised of a 4X buffered Fourier domain mode locked (FDML) [16] laser with an A-scan rate of ~1.5 MHz, central wavelength of 1316 nm, and bandwidth of 100 nm. A 7.3 kHz resonant scanner was utilized to rapidly scan the OCT probe beam across the sample. During the Appl-OCE measurement, the OCT probe beam was continuously scanned in a line across the apex of the corneas (B-M-mode imaging) [17]. Because the number of A-scans in each B-scan was divisible by 4, which was also the buffering factor of the FDML source, the same buffered sweep was used for each spatial position over time, enabling a phase stability of ~14 nm, measured in the cornea [18].

The IOP measurement technique is similar to that used by traditional noncontact tonometers [19]. A large displacement in the cornea with an air-puff produced by a rotary solenoid and plunger as seen in Fig. 2(a). During the inwards and outwards processes, there are times when the cornea is applanated (flat), such as at 1.4 ms and 15.3 ms after the air-puff in Fig. 2(a). We assume that at this position the force on the anterior surface of the cornea (i.e. the air-puff) equals the force on the posterior surface of the cornea (i.e. the IOP). These times when the cornea is applanated were then correlated to a measured temporal pressure profile of the air-puff. Due to the high frame rate of the PhS-OCT system, this dynamic process was imaged directly without any need for reconstruction or multiple excitations for a given measurement. However, three measurements were taken at each IOP for each sample to ensure repeatability and accuracy in the results. For comparison, IOP measurements were also made on the same samples with a commercially available rebound tonometer (TonoVet). Here, 5 repeated measurements were taken for each sample at each IOP.

The stiffness of the cornea was quantified by inducing a low amplitude (< 10 μm) elastic wave in the cornea with a focused micro air-pulse [20, 21], which was then imaged directly by the ultrafast PhS-OCT system [17], again with a single shot and no need for multiple excitations as with previous methods. Four measurements were made for each IOP and on each sample. The propagation of the elastic wave is displayed at selected times after excitation in Fig. 2(b). The elastic wave group velocity was then quantified by a cross-correlation based algorithm [22]. The elastic wave propagation delays, as computed by cross-correlation, were linearly fitted to the corresponding elastic wave propagation distances to compute the group velocity. The group velocity was then translated to Young's modulus with the surface wave equation [23].

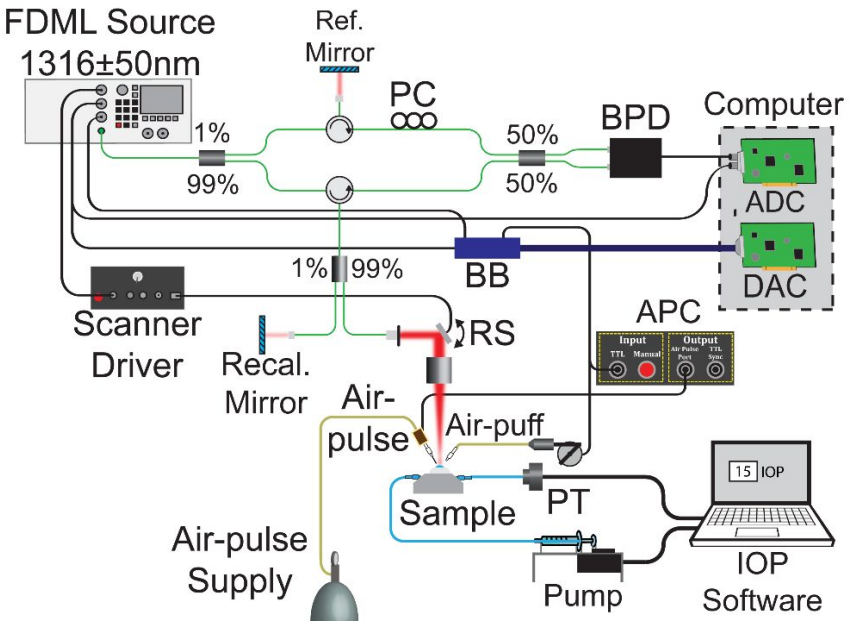

Figure 1. Schematic of the experimental setup. ADC: analog to digital converter; APC: air-pulse controller; BB: BNC board; DAC: digital to analog converter; PC: polarization controller; PT: pressure transducer; RS: resonant scanner.

3. RESULTS

The results of the IOP measurements are plotted in Figure 3(a). At the artificially controlled IOPs of 10, 15, and 20 mmHg, Appl-OCE measured the eye-globe IOP as 7.9±2.4, 13.4±0.2, and 21.3±2.0 mmHg, respectively. The rebound tonometer measured the IOP as 5.9±2.5, 11.1±2.2, and 17.7±2.0 mmHg at 10, 15, and 20 mmHg as set by the IOP control system, respectively. Paired t-tests were performed on the IOP as measured by Appl-OCE and as measured by the rebound tonometer against the artificially controlled IOP. The results showed that the IOP measured by Appl-OCE was not significantly different (P=0.85) from the artificially set IOP. However, the IOP measured by the rebound tonometer was significantly different (P<0.001). The elasticity of the corneas as a function of artificially controlled IOP is plotted in Fig. 3(b). The Young's moduli at 10, 15, 20 mmHg were 14.5±2.3, 50.0±2.0, and 158.8±31.8 kPa, respectively. The thickness of the cornea was also measured from the OCT structural image when there was no excitation, either from the air-puff or focused micro air-pulse. Using a constant refractive index of 1.376 [24], the central corneal thickness (CCT) at 10, 15, and 20 mmHg was 917±38, 1085±59, and 1064±25 μm.

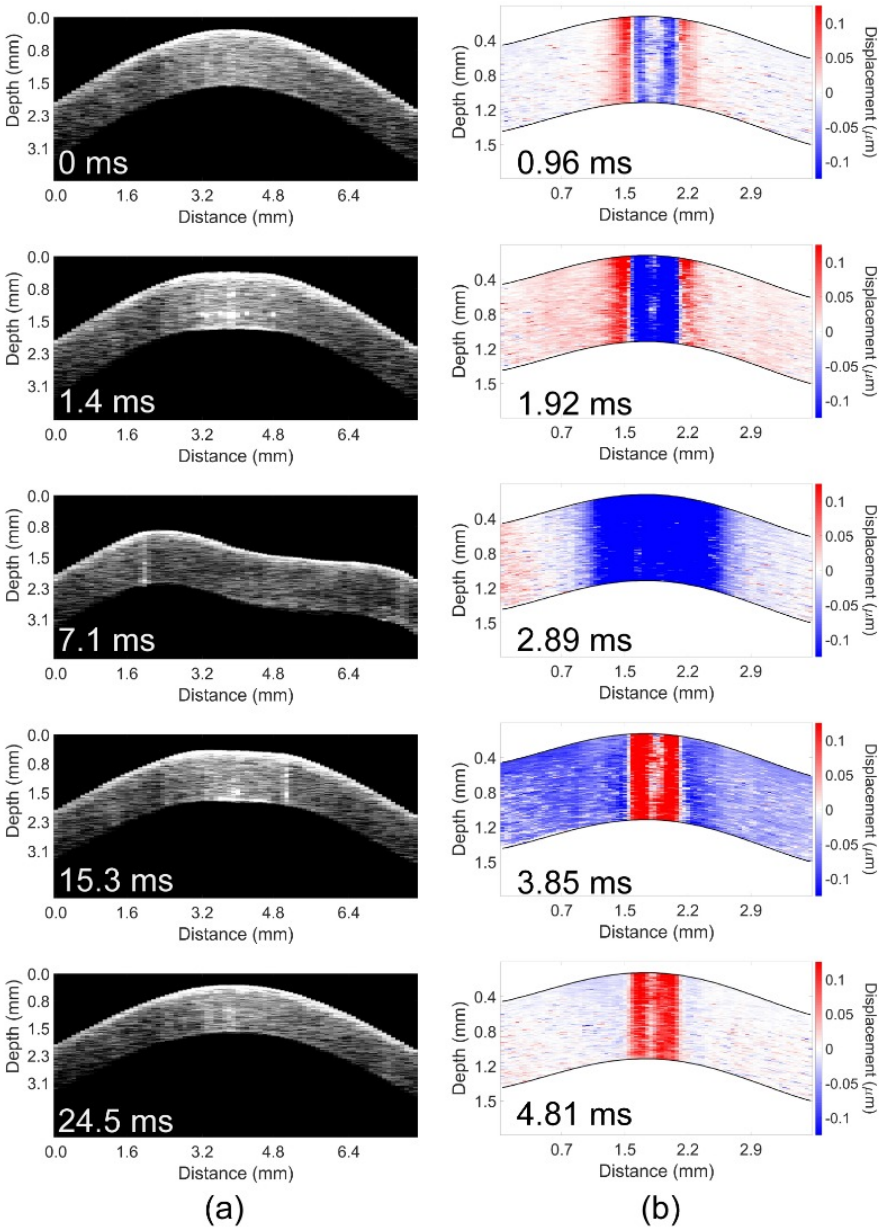

Figure 2. (a) Applanation of a porcine cornea at an artificially controlled IOP of 10 mmHg at the indicated times after the air-puff stimulation. (b) Propagation of the air-pulse induced elastic wave in the same porcine cornea at 10 mmHg at the indicated times after air-pulse excitation.

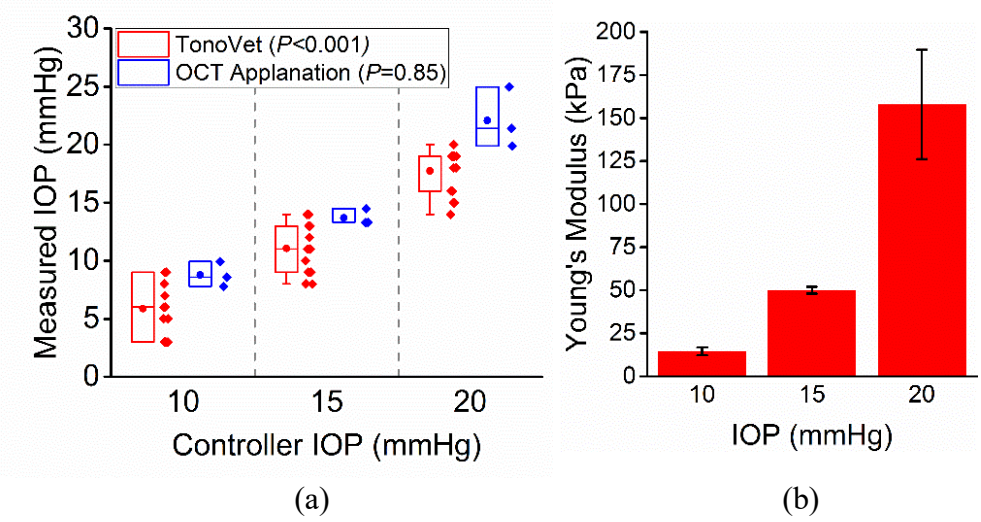

Figure 3. (a) IOP measurement by Appl-OCE and a commercially available rebound tonometer (TonoVet). Paired t-tests were performed to determine if the measured IOP was significantly different from the artificially controlled IOP, and the results are indicated in the graph legend. (b) The Young's modulus of the corneas as a function of IOP as quantified by the surface wave equation and Appl-OCE measured elastic wave group velocity. The *P* values of paired t-tests comparing the OCT-measured and rebound tonometer (TonoVet) IOP measurements to the artificially set IOP are indicated.

4. CONCLUSIONS AND FUTURE WORK

The presented Appl-OCE technique was able to measure changes in corneal geometry and stiffness as a function of IOP. Furthermore, Appl-OCE enabled measurement of the eye-globe IOP, and thus, may be useful as a screening device for ocular diseases due to its noncontact nature, high spatial and temporal resolutions, and need for only a single instrument. Our future work will involve building a more compact system, utilize a more robust elastic wave model, and the development of higher frequency excitations to minimize the influence of boundary conditions.

ACKNOWLEDGEMENTS

This work was supported, in part, by the U.S. National Institutes of Health (NIH) Grant Nos. 2R01EY022362, 1R01HL120140, and U54HG006348 and U.S. Department of Defense (DOD) Congressionally Directed Medical Research Programs (CDMRP) Grant No. PR150338.

REFERENCES

[1] D. P. Piñero, "Screening for eye disease: Our role, responsibility and opportunity of research," Journal of Optometry, 6(2), 67-68 (2013).
[2] P. R. Healey, [Screening for Glaucoma] Elsevier Saunders, London, 2 (2015).
[3] V. Mas-Tur, C. MacGregor, R. Jayaswal *et al.*, "A review of keratoconus: diagnosis, pathophysiology and genetics," Surv Ophthalmol, (2017).
[4] J. Li, Z. Han, M. Singh *et al.*, "Differentiating untreated and cross-linked porcine corneas of the same measured stiffness with optical coherence elastography," J Biomed Opt, 19(11), 110502 (2014).

[5] J. Liu, and X. He, "Corneal stiffness affects IOP elevation during rapid volume change in the eye," Invest Ophthalmol Vis Sci, 50(5), 2224-9 (2009).
[6] J. Liu, and C. J. Roberts, "Influence of corneal biomechanical properties on intraocular pressure measurement: quantitative analysis," J Cataract Refract Surg, 31(1), 146-55 (2005).
[7] F. A. Medeiros, and R. N. Weinreb, "Evaluation of the influence of corneal biomechanical properties on intraocular pressure measurements using the ocular response analyzer," J Glaucoma, 15(5), 364-70 (2006).
[8] J. Ophir, I. Cespedes, H. Ponnekanti *et al.*, "Elastography: a quantitative method for imaging the elasticity of biological tissues," Ultrason Imaging, 13(2), 111-34 (1991).
[9] R. Muthupillai, D. J. Lomas, P. J. Rossman *et al.*, "Magnetic resonance elastography by direct visualization of propagating acoustic strain waves," Science, 269(5232), 1854-7 (1995).
[10] J. M. Vaughan, and J. T. Randall, "Brillouin scattering, density and elastic properties of the lens and cornea of the eye," Nature, 284(5755), 489-91 (1980).
[11] G. Scarcelli, and S. H. Yun, "Confocal Brillouin microscopy for three-dimensional mechanical imaging," Nat Photonics, 2(1), 39-43 (2007).
[12] D. Huang, E. A. Swanson, C. P. Lin *et al.*, "Optical coherence tomography," Science, 254(5035), 1178-81 (1991).
[13] J. Schmitt, "OCT elastography: imaging microscopic deformation and strain of tissue," Opt Express, 3(6), 199-211 (1998).
[14] K. V. Larin, and D. D. Sampson, "Optical coherence elastography - OCT at work in tissue biomechanics [Invited]," Biomed Opt Express, 8(2), 1172-1202 (2017).
[15] M. D. Twa, J. Li, S. Vantipalli *et al.*, "Spatial characterization of corneal biomechanical properties with optical coherence elastography after UV cross-linking," Biomed Opt Express, 5(5), 1419-27 (2014).
[16] R. Huber, M. Wojtkowski, and J. G. Fujimoto, "Fourier Domain Mode Locking (FDML): A new laser operating regime and applications for optical coherence tomography," Opt Express, 14(8), 3225-37 (2006).
[17] M. Singh, C. Wu, C. H. Liu *et al.*, "Phase-sensitive optical coherence elastography at 1.5 million A-Lines per second," Opt Lett, 40(11), 2588-91 (2015).
[18] S. Song, W. Wei, B. Y. Hsieh *et al.*, "Strategies to improve phase-stability of ultrafast swept source optical coherence tomography for single shot imaging of transient mechanical waves at 16 kHz frame rate," Appl Phys Lett, 108(19), 191104 (2016).
[19] K. J. Myers, and C. A. Scott, "The non-contact ("air puff") tonometer: variability and corneal staining," Am J Optom Physiol Opt, 52(1), 36-46 (1975).
[20] S. Wang, K. V. Larin, J. S. Li *et al.*, "A focused air-pulse system for optical-coherence-tomography-based measurements of tissue elasticity," Laser Phys Lett, 10(7), 075605 (2013).
[21] S. Wang, and K. V. Larin, "Shear wave imaging optical coherence tomography (SWI-OCT) for ocular tissue biomechanics," Opt Lett, 39(1), 41-4 (2014).
[22] S. Wang, A. L. Lopez, 3rd, Y. Morikawa *et al.*, "Noncontact quantitative biomechanical characterization of cardiac muscle using shear wave imaging optical coherence tomography," Biomed Opt Express, 5(7), 1980-92 (2014).
[23] Z. Han, J. Li, M. Singh *et al.*, "Quantitative methods for reconstructing tissue biomechanical properties in optical coherence elastography: a comparison study," Phys Med Biol, 60(9), 3531-47 (2015).
[24] R. B. Mandell, "Corneal power correction factor for photorefractive keratectomy," J Refract Corneal Surg, 10(2), 125-8 (1994).